

SEARCHING FOR LUNAR HORIZON GLOW WITH THE LUNAR ORBITER LASER ALTIMETER.

M. K. Barker¹, E. Mazarico¹, D. E. Smith², X. Sun¹, M. T. Zuber², T. P. McClanahan¹, G. A. Neumann¹, M. H. Torrence³, J. W. Head⁴. ¹Solar System Exploration Division, NASA Goddard Space Flight Center 8800 Greenbelt Rd. Greenbelt, MD 20771, michael.k.barker@nasa.gov. ²Dept. of Earth, Atmospheric and Planetary Sciences, MIT, 77 Massachusetts Ave. Cambridge, MA 02139. ³Stinger Ghaffarian Technologies, Inc., 7701 Greenbelt Road, Suite 400, Greenbelt, Maryland 20770, USA. ⁴Dep. Earth, Env. & Planet. Sci., Brown Univ., Providence, RI, 02906, USA.

Introduction: Dust transport on the Moon affects many aspects of lunar surface science, such as the modification of small craters, rock burial and exposure, and track dating of grains. Moreover, as we learned from the Apollo program, dust is one of the largest obstacles to successful human exploration on the Moon. One observable phenomenon that could yield constraints on dust transport processes is scattered sunlight from exospheric dust grains. The brightest measurements of this lunar horizon glow (LHG) come from Apollo 15 coronal photographs taken from the Command Module near the surface dawn terminator around the time of a relatively active meteor stream [1,2]. A variety of other measurements have since placed limits on the dust density orders of magnitude below that inferred from Apollo 15 [3,4,5,6]. However, these more recent studies did not observe altitudes < 20 km during any major meteor streams. At altitudes > 20 km, LADEE-LDEX did measure enhanced dust impact rates during a few major streams [5]. Taken together, these results raise new questions on the temporal and spatial variability of the dust environment, and the role of meteor streams in producing Apollo 15-like LHG, the answers to which have implications for dust transport processes and planetary exploration in general.

To address these questions, we are conducting a campaign to search for LHG with the Laser Ranging (LR) system of the Lunar Orbiter Laser Altimeter (LOLA) aboard the Lunar Reconnaissance Orbiter (LRO). Advantages of this LOLA LHG search include (1) the LOLA-LR telescope can withstand direct sunlight allowing small elongation angles to be probed at any time of the year, (2) a long time baseline and regular sampling including meteor stream periods improves the chances of detecting LHG especially if it is an episodic phenomenon, and (3) the observations target a region of parameter space largely unconstrained in previous studies: meteor stream periods at altitudes < 20 km and elongation angles < 7°, thus more closely reproducing the conditions under which the Apollo 15 measurements were made. In this contribution, we describe the instrument, methodology, and some preliminary results.

Instrument: The LOLA instrument has 5 separate detectors, or channels, each dedicated to one of the 5 laser spots that comprise the LOLA footprint on the lunar surface [7]. The returned pulses from the foot-

print are collected by the LOLA receiver telescope. Each detector also records the background noise counts, which are proportional to the number of photons collected over an integration time of 0.0357 sec. It is these background counts that we use in this study by lowering the detection thresholds to allow LOLA to act as a radiometer. As part of the one-way LR experiment between Earth stations and LRO [8], Channel 1 is also connected via fiber optic cable to a second telescope mounted on, and co-aligned with, the LRO high gain antenna (HGA). The light collected by this LR telescope, with a 1.75° field-of-view (FOV), is fed through a 0.3-nm-wide bandpass filter centered on 532 nm.

Method: During a typical horizon observation, or scan, LRO performs a multi-axis slew so that the HGA and LR telescope are pointed at the limb for several minutes before/after sunrise/sunset. At sunrise/sunset, the Sun is usually within or just outside the LR FOV and, thus, a typical scan probes a range of elongation angles, tangent point altitudes, and distances to the terminator. The LR FOV is usually ~ 10 - 20 km wide at the horizon yielding typical tangent point altitudes < 20 km. Because of LRO's polar orbit, these observations tend to occur at high latitude, but as the β angle (the angle between the Sun and LRO's orbital angular momentum vector) shifts throughout the year, there are periods when they occur closer to the equator. The photometric calibration to solar brightness units (B_{sun}),

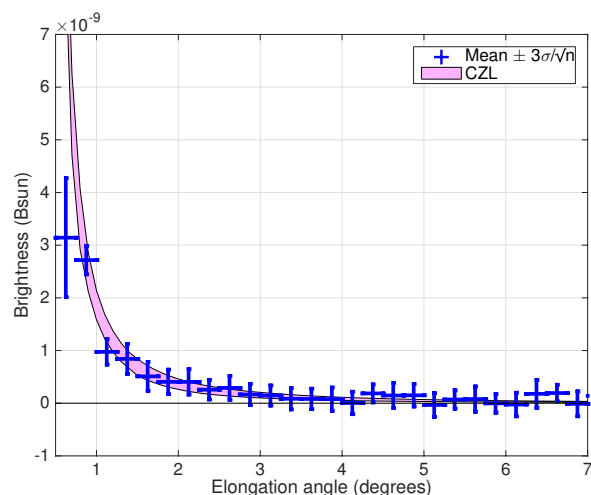


Figure 1 - Average brightness measurements for all scans. There is consistent observation of CZL.

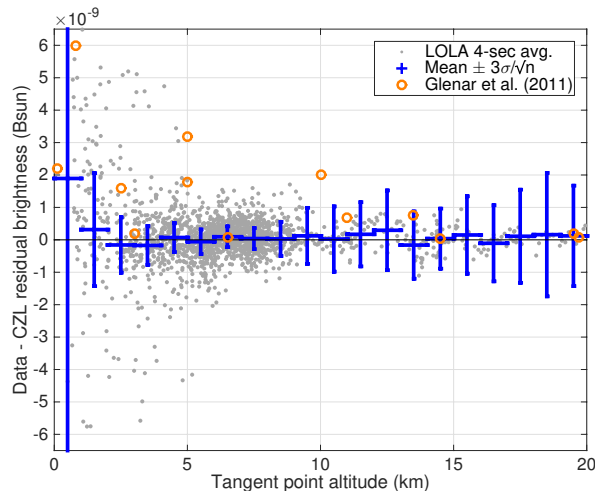


Figure 2 - (Data - CZL) residuals vs. tangent point altitude. There is no clear trend in the residuals as would be expected for a permanent lunar dust signal.

the mean brightness of the solar disk) is achieved by fitting the data from the scan on 2016 DOY 099 to SOHO/LASCO C2 and C3 images of the coronal and zodiacal light (CZL) taken on the same day. A constant CZL model to compare to all scans is constructed from the minimum of 24 LASCO images taken at regular intervals in 2005 (at about the same point in the solar cycle). As of Nov. 30, 2017, 62 total limb scans were successfully conducted (35 dawn, 27 dusk, 24 stream). The meteor streams sampled were the Southern Delta Aquariids, Perseids, Leonids, Geminids, and Quadrantids.

Results: Stacking the data from all the scans together reveals a trend with elongation angle consistent with the CZL (Figure 1). How much room does this leave for an LHG component? The observed signal is, in general, a function of elongation angle and sky visibility within the FOV (i.e., the fraction of the FOV that is unobscured by topography). To estimate the sky visibility, we sub-sample the FOV with 500 sightlines and determine whether each sightline intersects the lunar surface of the 64 PPD LOLA shape model, and if not, what CZL value it would measure. To boost the signal-to-noise ratio, we average the full rate data into 4-sec bins with ~ 100 points per bin. The resulting residuals (data - CZL) are divided by the visibility to normalize them to the full FOV. These normalized residuals (Figure 2) show no clear trend with tangent point altitude as would be expected for an Apollo 15-like LHG (orange circles [2]). Mie theory and a log-normal dust grain size distribution (peak radius of $0.1 \mu\text{m}$) give the predicted line-of-sight (LOS) dust grain radiance [4], which then yields an average dust LOS column density $N = (0.2 \pm 4) \times 10^4 \text{ cm}^{-2}$. This is consistent with no dust, and there is no significant difference between the

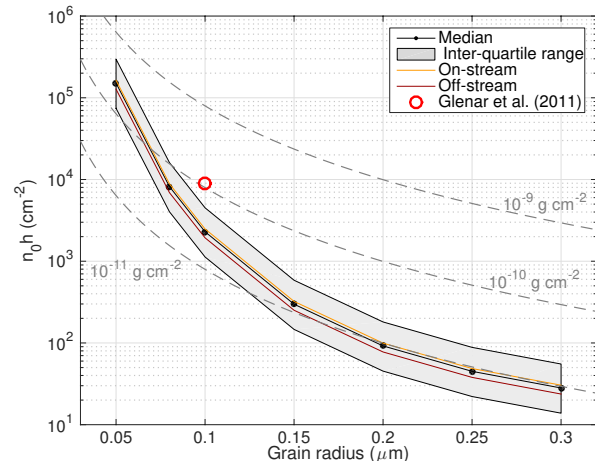


Figure 3 - Dust upper limits vs. grain radius. Black dots show the median upper limit on the vertical column density ($n_0 h$) near the terminator. The shaded region is the interquartile range of upper limits. There is no significant difference between the on-stream and off-stream sub-samples. Assuming a lunar-like particle volume mass density of 3 g cm^{-3} , dashed gray lines show lines of constant vertical column mass density, which is less dependent on grain radius than $n_0 h$.

total sample and on-stream and off-stream sub-samples.

We can also place limits on the vertical dust column density near the terminator by assuming a 1-D vertically decreasing exponential dust concentration profile. For each scan, we compute the integrated radiance from all illuminated grains along each of the 500 sightlines, accounting for the varying altitude and dust concentration along each sightline due to distance and topography. Because our spatial resolution at the limb is typically around 10 km, we can only place upper limits on the vertical column density, $n_0 h$, the product of the surface dust concentration, n_0 , and exponential scale height, h . Most of the dust upper limits (black points and shaded region in Figure 3) are $\sim 3x$ lower than the Apollo 15 estimate (red circle [2]). As before, the off-stream and on-stream samples are not significantly different. Altogether, these results suggest that, if real, Apollo 15-like LHG is not a sustained or common occurrence during meteor stream periods.

References: [1] McCoy J. E. (1976) *Proc. Lunar Sci. Conf. VII*, 1087-1112. [2] Glenar D. A. et al. (2011) *Planet. Space Sci.*, 59, 1695-1701. [3] Feldman P. D. et al. (2014) *Icarus*, 233, 106-113. [4] Glenar et al. (2014) *J. Geophys. Res. Planets*, 119, 2548-2567. [5] Horanyi, M. et al. (2015) *Nature*, 522, 324-326. [6] Szalay, J. & Horanyi, M. (2015) *GRL*, 42, 5141-5146. [7] Smith D. E. et al. (2017) *Icarus*, 283, 70. [8] Mao, D. et al. (2017) *Icarus*, 283, 55.